An Alternative Mechanism for the Dimerization of Formic Acid

Nicole R. Brinkmann,[†] Gregory S. Tschumper,[‡] Ge Yan,[†] and Henry F. Schaefer, III*,[†]

Center for Computational Quantum Chemistry, University of Georgia, Athens, Georgia 30602-2525, and Department of Chemistry and Biochemistry, University of Mississippi, University, Mississippi 38677

Received: August 31, 2003

Gas-phase formic acid exists primarily as a cyclic dimer. The mechanism of dimerization has been traditionally considered to be a synchronous process; however, recent experimental findings suggest a possible alternative mechanism by which two formic acid monomers proceed through an acyclic dimer to the cyclic dimer in a stepwise process. To investigate this newly proposed process of dimerization in formic acid, density functional theory and second-order Møller−Plesset perturbation theory (MP2) have been used to optimize cis and trans monomers of formic acid, the acyclic and cyclic dimers, and the acyclic and cyclic transition states between minima. Single-point energies of the trans monomer, dimer minima, and transition states at the MP2/TZ2P+diff optimized geometries were computed at the coupled-cluster level of theory including singles and doubles with perturbatively applied triple excitations [CCSD(T)] with an aug′-cc-pVTZ basis set to obtain an accurate determination of energy barriers and dissociation energies. A counterpoise correction was performed to determine an estimate of the basis set superposition error in computing relative energies. The explicitly correlated MP2 method of Kutzelnigg and Klopper (MP2-R12) was used to provide an independent means for obtaining the MP2 one-particle limit. The cyclic minimum is predicted to be 6.3 kcal/mol more stable than the acyclic minimum, and the barrier to double proton transfer is 7.1 kcal/mol.

Introduction

Proton transfer is one of the simplest and most fundamental reactions in chemistry. As such, it has been studied extensively, both experimentally[1−5] and theoretically.[6−8] However, most of these studies have been for reactions in which a single proton is transferred. Reactions having multiple proton transfers have not been studied exhaustively. Examples of multiproton transfer include proton relay systems in enzymes and certain proton-transfer processes in hydrogen-bonded water complexes. Kinetic isotope effects involving the double proton transfer in oxalamidines,[9,10] bis(*p*-fluorophenyl)formamidine,[11] and acetylporphyrin[12] have been studied computationally using ^{1}H, ^{13}C, and ^{19}F NMR where applicable. Multiple proton-transfer reactions in solution have been studied using molecular dynamics simulations.[13] In particular, Kohanoff and co-workers used a hybrid quantum mechanical−molecular mechanical method to address issues such as how thermal and solvent fluctuations couple with the motion of protons, the "degree of concertedness" in the multiple proton transfer, and relevant time scales. The potential energy surface of the double proton transfer in the adenine−thymine base pair was studied theoretically using second-order Møller−Plesset perturbation theory with a double-ζ basis set.[14] Hobza and co-workers reported that the character of the theoretically constructed potential energy surface for the double proton transfer depends strongly on the level of theory and the size of the basis set used. Systems of biological interest that exhibit double proton transfer include dimeric ibuprofen, crystalline benzoic acid, and a protein embedded in a membrane. Because these molecules are large, even computations utilizing moderate basis sets present a challenge, and the more extensive basis sets for such systems are colossal. Thus a small system having multiple hydrogen bonds is desirable.

The carboxyl functional group (−COOH) is a fundamental building block of amino acids and has been the subject of several conformational analysis studies, both theoretical and experimental. Theoretical studies[15−17] have confirmed that hydrogen bonding is a factor affecting the conformational energetics of simple neutral amino acids. In 1992, Császár[15] used second-, third-, and fourth-order Møller−Plesset perturbation theory (MP2, MP3, and MP4) and coupled-cluster methods including single and double excitations (CCSD) and perturbatively applied triples [CCSD(T)] with a 6-311++G** basis set to investigate the hydrogen bonding in gaseous glycine. In 1996, he studied α-alanine and formic acid using MP2 with Pople's split-valence basis sets and also the correlation-consistent, polarized-valence basis sets (cc-pVTZ, aug-cc-pVTZ, and cc-pVQZ) of Dunning and co-workers. Formic acid is the simplest neutral compound containing a carboxyl group. While crystalline formic acid is characterized by long catameric chains linked by O−H···O hydrogen bonds,[18,19] gas-phase formic acid can exist in monomeric form but more predominantly as cyclic, doubly hydrogen-bonded dimers.[20−22]

The formic acid monomer (FAM) exists in both cis and trans isomers (Figure 1); the notation from the original experimental work of Hocking,[23] which designates *cis*-FAM as the stereoisomer with hydrogen atoms cis to one another, is also employed here. The cis isomer is less stable than the trans isomer by 3.90 ± 0.09 kcal/mol[23] and has a much larger dipole moment (3.79 vs 1.42 D).[24] Microwave spectra have provided geometrical parameters, and the barrier to rotation about the C−OH bond was reported as 13.8 kcal/mol.[25] Normal-mode analyses led to assignments of the fundamental vibrational frequencies.[26−28] In 1998, the total energies of the cis and trans isomers of FAM were computed using MP2, MP3, MP4, MP5, CCSD, CCSD(T),

* To whom correspondence should be addressed. E-mail: hfsiii@arches.uga.edu.
[†] University of Georgia.
[‡] University of Mississippi.

10.1021/jp031043f CCC: $25.00 © 2003 American Chemical Society
Published on Web 11/01/2003

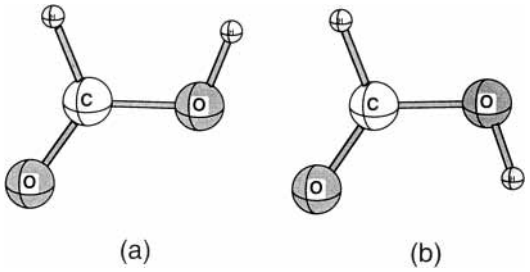

Figure 1. Schematic diagrams of (a) *cis*- and (b) *trans*-formic acid (C_s).

and CCSDT with cc-pVXZ and aug-cc-pVXZ (where X = D, T, Q, 5, and 6) at the cc-pVTZ CCSD(T) optimized geometry.[29]

The formic acid dimer (FAD) is the simplest homodimer for which the structure of the molecule at the global minimum of the potential energy surface is cyclic. Because of this characteristic and because each FAM moiety acts as both a hydrogen bond donor and acceptor, FAD is an ideal prototype for studying multiproton transfer. The cyclic structure of the dimer was determined using electron diffraction by Almenninger, Bastiansen, and Motzfeld,[21] and the approximate geometrical dimensions of the ring were determined by Costain and Srivastava[30] in 1964. The IR and Raman frequencies of FAD were measured by Bertie, Michaelian, and Eysel[31,32] and by Millikan and Pitzer.[33] Early studies of FAD focused on the geometrical changes upon dimerization and the energetics of stabilization due to the hydrogen bonds in the dimer.[22,34,35] More recent theoretical studies using ab initio quantum chemical methods at various levels of theory have focused not only on the structure of the cyclic dimer but also on other regions of the potential energy surface,[36,37] and the binding energy of FAD was predicted to be 13.9 kcal/mol by Tsuzuki and co-workers who used MP2 theory with the cc-pVXZ basis sets up through 5Z and an extrapolation scheme.[38]

Until recently, examination of the double proton transfer in FAD has been based on a one-dimensional double well potential.[39,40] In these studies, a single transition-state structure with D_{2h} symmetry was found, which suggests that the double proton transfer in FAD has only one transition state and that dimerization proceeds through a concerted mechanism,[37] along the minimum energy path of which the structure of FAD maintains C_{2h} symmetry. The barrier height of the multiple proton transfer in FAD was reported in 1996 to be 8.9 kcal/mol at the G* level of theory.[41]

However, new findings suggest that before the double proton transfer occurs in the cyclic minimum, formic acid dimerizes in a stepwise mechanism.[42] Gantenberg, Halupka, and Sander isolated FAM in an argon matrix, and upon warming the matrix from 7 to 40 K, they found that formic acid dimerized in an "open" dimer (Figure 2a). Upon further warming of the matrix, the acyclic C_s dimer closed to form the C_{2h} dimer (Figure 2b). An acyclic transition state between the acyclic and cyclic dimers might be expected in a stepwise mechanism of this nature.

Because proton transfer plays an integral role in many chemical and biological systems, the knowledge of the total energies and geometrical parameters of hydrogen-bonded species is important to the understanding of such dynamical systems. While several other dimeric conformations composed of cis- and trans-FAM exist on the formic acid potential energy surface,[8,43] the global minimum is the cyclic structure examined in this study, and the acyclic dimer reported experimentally[42] is the singly hydrogen-bonded dimer considered here. In this study, we used high-level ab initio methods to investigate the

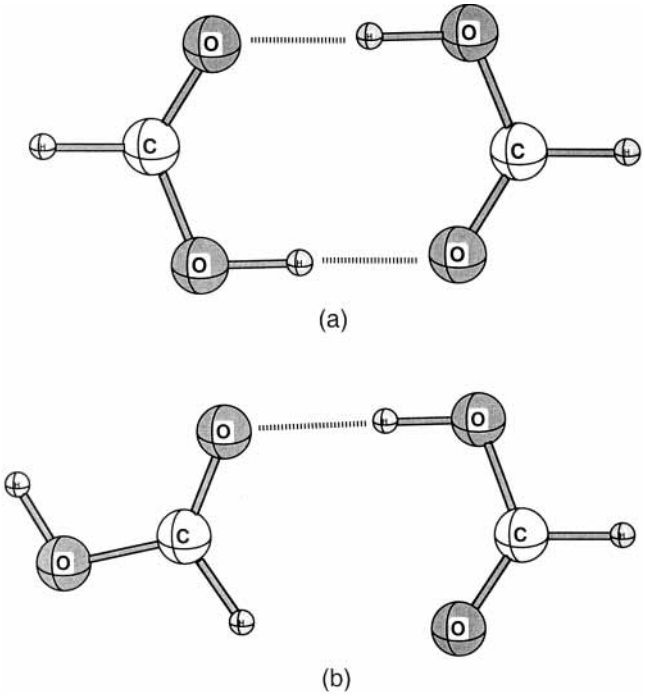

Figure 2. Formic acid dimer in (a) C_{2h} symmetry and (b) C_s symmetry.

optimized structures of the formic acid monomer (cis and trans), acyclic C_s dimer, cyclic C_{2h} dimer, acyclic C_1 transition state, and cyclic D_{2h} transition state and to compute the harmonic vibrational frequencies of these systems to verify whether the stationary points are minima or transition states. However, the primary purpose of this study was to employ higher levels of ab initio theories and methods than ever previously used to definitively establish the dissociation energy of the equilibrium cyclic dimer and the barrier height for the double proton transfer process, the barrier to ring opening from the cyclic dimer to the acyclic dimer, and the binding energy of the acyclic dimer. Because the theoretical results of such a system are sensitive to the size of the basis set and the level of theory used, the basis set and correlation effects have been treated systematically to determine the relative energies and barrier heights to within 1 kJ/mol.

Theoretical Methods

All quantum mechanical computations were carried out with the Gaussian 94,[44] ACESII,[45] and NWChem[46] ab initio program packages. Three basis sets were used for the optimizations of the cis and trans isomers of the formic acid monomer, the acyclic C_s dimer (a-FAD), cyclic C_{2h} dimer (c-FAD), acyclic C_1 transition state, and the cyclic D_{2h} transition state.

The smallest basis set was a double-ζ plus polarization and diffuse functions (DZP+diff) basis. This basis set was constructed from the Huzinage−Dunning[47,48] set of contracted double-ζ Gaussian functions. Added to this was one set of *p*-type polarization functions for each H atom and one set of five *d*-type polarization functions for each C and O with orbital exponents $\alpha_p(H) = 0.75$, $\alpha_d(C) = 0.85$, and $\alpha_d(O) = 0.85$. To complete the DZP+diff basis, the entire set of functions was augmented with one "even-tempered"[49] *s* diffuse function for each H atom and one set of "even-tempered" *s* and *p* diffuse functions for each C and O atom with orbital exponents determined by the formula expressed by Lee and Schaefer[49,50] [$\alpha_s(H) = 0.044\,15$, $\alpha_s(C) = 0.043\,02$, $\alpha_p(C) = 0.036\,29$, $\alpha_s(O) = 0.082\,27$, $\alpha_p(O) = 0.065\,08$]. The final contraction scheme for this basis is H(5s1p/3s1p) and C,O(10s6p1d/5s3p1d).

The second basis set was a triple-ζ plus polarization and diffuse functions (TZ2P+diff) basis. The H(5s1p/3s1p) and C,O(10s6p/5s3p) contracted triple-ζ Gaussian functions of Dunning[51] were augmented with two sets of *d* polarization functions for each C and O atom with orbital exponents $\alpha_d(C) = 1.50$ and 0.375 and $\alpha_d(O) = 1.70$ and 0.425. One set of "even-tempered" *s* and *p* diffuse functions were added for each atom [$\alpha_s(H) = 0.030\,16$, $\alpha_p(H) = 0.375\,00$, $\alpha_s(C) = 0.048\,12$, $\alpha_p(C) = 0.033\,89$, $\alpha_s(O) = 0.089\,93$, $\alpha_p(O) = 0.058\,40$]. The final contraction scheme for the TZ2P+diff basis set is H(6s2p/4s2p) and C,O(12s7p2d/6s4p2d).

The largest basis set used for the optimizations was the triple-ζ plus two sets of polarization functions and one set of diffuse functions augmented with *d* and *f* polarization functions [TZ2P(f,d)+diff]. This basis set was constructed in the same manner as the TZ2P+diff basis, but it was augmented with one set of *d* polarization functions for each H atom and two sets of *d* and one set of *f* polarization functions for each C and O atom with orbital exponents $\alpha_d(H) = 1.00$, $\alpha_d(C) = 1.50$ and 0.375, $\alpha_d(O) = 1.70$ and 0.425, $\alpha_f(C) = 0.80$, and $\alpha_f(O) = 1.40$. The final contraction scheme is H(6s2p1d/4s2p1d) and C,O(12s7p2d1f/6s4p2d1f).

Geometries were optimized using hybrid Hartree−Fock/density functional theory (DFT) and second-order Møller−Plesset perturbation theory (MP2).[52,53] The B3LYP functional, using Becke's three-parameter exchange functional (B3)[54] with the correlation functional of Lee, Yang, and Parr (LYP),[55] was used for the DFT computations. For each stationary point found, the harmonic vibrational frequencies were obtained from the analytic second derivatives available for the B3LYP functional.

Single-point energies for the trans monomer and dimers at the MP2/TZ2P+diff optimized geometries were obtained for the accurate determination of energy barriers and dissociation energies. These computations were performed at the coupled-cluster level of theory including singles and doubles with perturbatively applied triple excitations [CCSD(T)][56−59] with an aug′-cc-pVTZ basis set. The aug′-cc-pVTZ basis set was formed by adding one diffuse function for each value of angular momentum, *l*, to Dunning's correlation-consistent polarized triple-ζ basis set (cc-pVTZ)[60] for all heavy atoms (i.e., aug-cc-pVTZ[61] for C and O atoms and cc-pVTZ for H atoms). The final contraction scheme is H(5s2p1d/3s2p1d) and C,O(11s6p3d2f/524p3d2f).

The dissociation energy of the cyclic dimer was obtained as

$$D_e(\text{c-FAD}) = 2E_{\text{trans-FAM}} - E_{\text{c-FAD}}.$$

The barrier to the double proton transfer was calculated as

$$\Delta E^{\dagger}(\text{c-FAD}) = E^{\dagger}_{\text{c-FAD}} - E_{\text{c-FAD}}.$$

The binding energy of the acyclic dimer was computed from

$$D_e(\text{a-FAD}) = 2E_{\text{trans-FAM}} - E_{\text{a-FAD}}.$$

The barrier to ring opening was determined from

$$\Delta E^{\dagger}(\text{a-FAD}) = E^{\dagger}_{\text{a-FAD}} - E_{\text{a-FAD}}.$$

To obtain an estimate of the basis set superposition error (BSSE) in computing the dissociation energy in each of the proposed mechanisms, a counterpoise correction[62] was performed. The single-point energy of the monomer moiety in the cyclic dimer was computed by deleting the atomic centers of one moiety but leaving the basis functions for those centers. The notation $E^{B}_{G}(F)$ is introduced to denote the basis set (B) and geometry (G) used to compute the energy of fragment F. The uncorrected D_e is merely the energy of two monomers (A = B) minus the energy of the dimer (AB).

$$D_e = 2E^{A}_{A}(A) - E^{AB}_{AB}(AB) \quad (1)$$

The correction for BSSE allows the monomers to utilize the basis functions available in the dimer and compensates for relaxation effects.

$$D^{CP}_{e} = E^{AB}_{AB}(A) + E^{AB}_{AB}(A) - E^{AB}_{AB}(AB) - (E^{A}_{AB}(A) - E^{A}_{A}(A)) - (E^{B}_{AB}(B) - E^{B}_{B}(B)) \quad (2)$$

Similar computations were made for each moiety of the acyclic dimer. These energy points were found using B3LYP and MP2 with the DZP+diff, TZ2P+diff, and TZ2P(f,d)+diff basis sets, as well as by using CCSD(T) with aug′-cc-pVTZ basis set.

The explicitly correlated MP2 method of Kutzelnigg and Klopper[63] (MP2-R12) provides an independent means for obtaining the MP2 one-particle limit. This is achieved by including explicit linear dependence on the interelectronic distances in the first-order correction to the reference wave function. Here we used the MP2-R12 method in standard approximation A[64] as implemented in the PSI3 program package.[65,66] The approximate resolution of the identity implicit in the MP2-R12/A method in its present formulation demands basis sets of near Hartree−Fock limit quality to be used in the computations. To this end, we use a specialized, uncontracted basis set, denoted K2, derived from Dunning's cc-pV5Z set by Klopper.[67] It is technically (15s9p7d5f) for carbon and oxygen atoms and (9s7p5d) for hydrogen atoms. Thus, the K2 MP2-R12/A correlation energy is adopted as an estimate for the one-particle limit of the MP2 correlation energy. A MP2 complete basis set (CBS) limit is then straightforwardly evaluated as a sum of the K2 MP2-R12/A correlation energy and the SCF CBS limit. In the remainder of this manuscript, MP2-R12/A will simply be referred to as MP2-R12.

Results and Discussion

A. Geometries. The geometrical parameters of FAM (cis and trans) were optimized at the B3LYP and MP2 levels of theory with three basis sets [DZP+diff, TZ2P+diff, and TZ2P(f,d)+diff]. The structures of the acyclic dimer, acyclic transition state, cyclic minimum, and cyclic transition state were also optimized at these levels of theory with the corresponding basis sets. These results are compiled in Table 1. Where available, experimental data is included for comparison. Harmonic vibrational frequencies for each structure were determined using the B3LYP method. All frequencies computed for the two isomers of FAM and for the acyclic and cyclic dimers were real, indicating that these structures are true minima. For the C_1 and D_{2h} structures, a single imaginary frequency was observed, confirming that these are transition state structures.

The bond distances and bond angles of *cis*- and *trans*-FAM reported in this study agree well with the experimentally reported geometrical parameters. More rigorous theoretical investigations of monomeric formic acid have been previously conducted, and interested readers are directed to refs 29 and 68−71.

The theoretically predicted and experimentally reported geometrical parameters of the C_{2h} cyclic dimer are given in Table 1, although direct comparisons should not be made between the theoretical r_e structure and the experimental vibrationally averaged r_0 structure. The C−H bond distance of

TABLE 1: The Optimized Geometrical Parameters of *trans*-Formic Acid Monomer (FAM), Cyclic and Acyclic Formic Acid Dimer (c-FAD and a-FAD), and the Cyclic and Acyclic Formic Acid Dimer Transition States (c-FAD† and a-FAD†)[a]

system	r(C−H)	r(C═O)	r(C−O)	r(O−H)	r(O···H)	θ(H−C═O)	θ(O═C−O)	θ(H−O−C)	θ(C═O···H)	θ(O···H−O)	τ(O−C═O···H)
trans-FAM[b]	1.097(5)	1.202(10)	1.343(10)	0.972(5)		124.1(2)	124.9(1)	106.3(1)			
DZP+diff	1.102	1.210	1.350	0.977		125.1	125.0	107.4			
TZ2P+diff	1.095	1.197	1.346	0.970		125.2	125.1	107.8			
TZ2P(f,d)+diff	1.091	1.203	1.347	0.969		125.2	125.1	106.4			
DZP+diff	1.099	1.218	1.356	0.978		125.3	125.1	106.3			
TZ2P+diff	1.090	1.205	1.351	0.969		125.2	125.1	106.5			
TZ2P(f,d)+diff	1.096	1.197	1.344	0.970		125.2	125.2	108.0			
c-FAD[c]	1.079(21)	1.217(3)	1.320(3)	1.320(17)		115.4(3.1)	126.2(1.0)	108.5(0.4)		180.0	
DZP+diff	1.101	1.231	1.314	1.013	1.628	121.5	126.2	110.5	125.0	178.3	
TZ2P+diff	1.094	1.218	1.311	1.001	1.672	121.8	127.4	110.8	124.2	178.7	
TZ2P(f,d)+diff	1.095	1.217	1.309	1.001	1.670	121.9	127.2	110.9	124.5	178.3	
DZP+diff	1.098	1.236	1.323	1.004	1.670	121.9	129.1	109.0	126.0	178.8	
TZ2P+diff	1.088	1.223	1.318	0.994	1.690	122.1	128.5	109.4	124.6	179.8	
TZ2P(f,d)+diff	1.090	1.222	1.313	0.998	1.663	122.0	126.3	109.4	124.4	179.9	
a-FAD											
						Moiety A					
DZP+diff	1.099	1.222	1.336	0.977		123.8	123.6	108.1			
TZ2P+diff	1.092	1.209	1.333	0.970		124.0	123.9	108.4			
TZ2P(f,d)+diff	1.093	1.209	1.331	0.971		124.0	123.9	108.6			
DZP+diff	1.096	1.229	1.343	0.978		124.1	123.7	106.8			
TZ2P+diff	1.087	1.216	1.338	0.969		124.0	123.9	107.1			
TZ2P(f,d)+diff	1.088	1.214	1.333	0.969		124.0	123.9	107.0			
						Moiety B					
DZP+diff	1.103	1.220	1.332	0.998	1.743	123.3	125.8	109.3	115.9	177.1	0.0
TZ2P+diff	1.096	1.207	1.328	0.989	1.777	123.6	125.9	109.5	115.7	177.1	0.0
TZ2P(f,d)+diff	1.097	1.093	1.326	0.989	1.777	123.6	125.9	109.7	116.1	176.6	0.0
DZP+diff	1.100	1.226	1.339	0.994	1.767	123.7	125.7	107.8	116.3	177.6	0.0
TZ2P+diff	1.090	1.213	1.334	0.985	1.777	123.7	125.8	108.2	115.3	178.8	0.0
TZ2P(f,d)+diff	1.092	1.212	1.329	0.987	1.763	123.7	125.8	108.1	115.3	178.1	0.0
c-FAD†											
DZP+diff	1.100	1.269		1.210			126.6	115.9		180.0	
TZ2P+diff	1.093	1.260		1.210			126.7	115.7		180.0	
TZ2P(f,d)+diff	1.094	1.259		1.211			126.7	116.7		180.0	
DZP+diff	1.097	1.274		1.205			126.7	115.3		180.0	
TZ2P+diff	1.088	1.265		1.206			126.8	116.6		180.0	
TZ2P(f,d)+diff	1.089	1.262		1.204			126.8	114.9		180.0	
a-FAD†											
						Moiety A					
TZ2P+diff	1.093	1.204	1.332	0.970		124.6	125.0	108.4			
TZ2P(f,d)+diff	1.094	1.204	1.330	0.971		124.7	125.0	108.6			
TZ2P+diff	1.088	1.212	1.336	0.969		124.6	125.0	107.1			
TZ2P(f,d)+diff	1.089	1.210	1.331	0.970		124.7	125.0	107.1			
						Moiety B					
TZ2P+diff	1.096	1.203	1.334	0.980	1.844	124.0	125.9	109.2	131.4	174.8	105.2
TZ2P(f,d)+diff	1.098	1.202	1.333	0.980	1.843	124.1	125.9	109.4	132.0	174.4	105.4
TZ2P+diff	1.091	1.211	1.340	0.977	1.847	124.2	125.8	107.7	125.1	170.6	101.8
TZ2P(f,d)+diff	1.092	1.209	1.335	0.979	1.835	124.2	125.8	107.6	124.0	170.4	101.6

[a] Experimentally reported parameters are in italics. DFT results are in lightface type, and MP2 results are in boldface type. Bond lengths are in Å, and bond angles are in degrees. [b] Reference 73. [c] Reference 21.

1.088 Å is not significantly different compared to the other monomer and dimer structures. The O−H bond distance is longer than that in FAM by about 0.02 Å and about 0.01 Å longer than that for the acyclic minimum, which is consistent with the participation of this hydrogen atom in the hydrogen bond. The C−O bond distance is ∼0.03 Å shorter than that in FAM and ∼0.02 Å shorter than that in the acyclic dimer. The C═O bond distance increased by about 0.02 and 0.01 Å as compared to that in FAM and the acyclic dimer, respectively. This observation is consistent with the doubly bonded O atom participating in the hydrogen bond. The H−O−C bond angle of 109.4° [MP2/TZ2P(f,d)+diff] was observed to be about 3° wider than that in FAM and 1° wider than that in acyclic FAD, while the H−C═O bond angle decreased by about 3° and 1°, respectively. The O−C═O bond angle is widest in the cyclic dimer, approximately 3.5° wider than that in FAM and 3° wider than that in acyclic FAD. The O···H hydrogen bond distance is predicted to be about 1.7 Å, and the O···H−O bond angle is almost perfectly linear at 179.9°.

The geometrical parameters of the C_s acyclic dimer (Figure 2a) are best analyzed in terms of the donor and acceptor monomer moieties. There was no significant change observed in the O−H bond distance in the acceptor upon dimerization. However, the O−H bond distance in the donor increased by ∼0.02 Å, because this H atom participates in the hydrogen-bond linkage between the two moieties of the dimer. The C−H bond decreased by ∼0.003 Å in the acceptor but experienced no significant change in the donor. The C−O bond distances decreased in the dimer (∼0.01 Å, acceptor; ∼0.02 Å, donor), while the C═O bond distances each increased by about 0.01 Å. The H−O−C bond angles increased in the dimer (∼1°, acceptor; ∼1.5°, donor), and the H−C═O bond angles decreased in both the acceptor and the donor by ∼0.6° and ∼1.7°, respectively. The O−C═O bond angle decreased in the acceptor

TABLE 2: Relative Electronic Energies in kcal/mol of the cis and trans Isomers of the Formic Acid Monomer (FAM), the Cyclic and Acyclic Minima of the Formic Acid Dimer (c-FAD, a-FAD), and the Cyclic and Acyclic Transition States of the Dimer (c-FAD†, A-FAD†)[a]

	B3LYP			MP2			MP2−R12	CCSD(T)
System	DZP+dif	TZ2P+dif	TZ2P(f,d)+dif	DZP+dif	TZ2P+dif	TZ2P(f,d)+dif	K2	aug′-cc-pVTZ
2(*trans*-FAM)	0.0	0.0	0.0	0.0	0.0	0.0	0.0	0.0
c-FAD	−16.47	−15.17	−15.18	−16.63	−15.87	−16.18	−16.09	−17.19 (−14.79)
a-FAD	−9.37	−8.51	−8.50	−10.36	−9.51	−9.63	−9.74	−9.67 (−9.06)
c-FAD†	−11.51	−8.38	−8.70	−10.25	−7.27	−9.40	−8.99	−8.11
a-FAD†	-	−5.61	−5.66	-	−6.71	−6.80	−6.88	−7.57

Zero-point corrected energies are listed in parentheses.

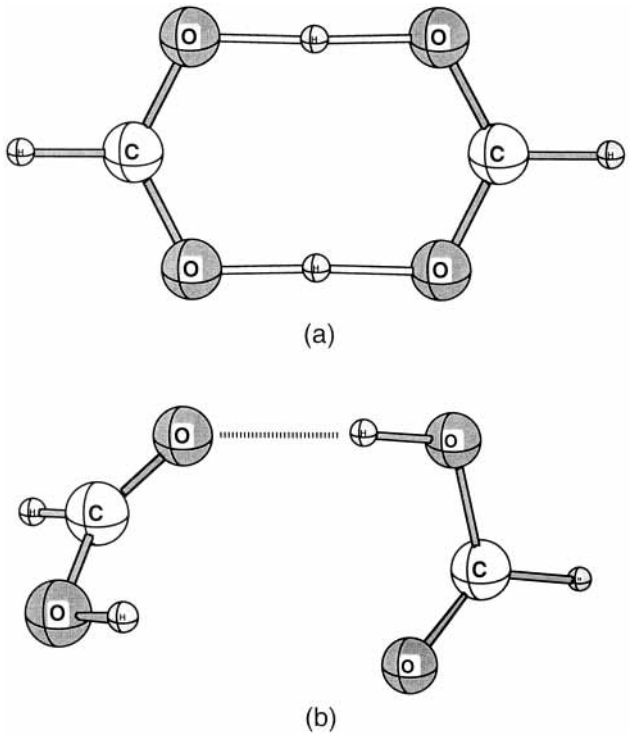

Figure 3. Transitions states of the formic acid dimer in (a) D_{2h} symmetry and (b) C_1 symmetry.

(∼1.3°) but increased in the donor (∼0.7°). At our best level, the O···H bond distance is predicted to be 1.763 Å, and the O···H−O bond angle is 178.1°.

The D_{2h} cyclic transition state (Figure 3a) is best compared to the FAM and C_{2h} FAD structures. The C−H bond distance (1.089 Å) experiences no significant change compared to that of FAM (1.089 Å) or C_{2h} FAD (1.090 Å). However, the O−H bond distance increases by about 0.2 Å as compared to both FAM and C_{2h} FAD. In this transition state, the C−O bonds are resonance hybrids between C−O single and C═O double bonds. Thus, it is not surprising that the predicted value of this parameter (1.262 Å) is approximately an average of the C−O (1.344 Å) and C═O (1.197 Å) bond distances of FAM. Similarly, the H−C−O bond angle is a resonance hybrid between the H−C═O and H−C−O bond angles of the cyclic dimer, and this parameter (114.9°) is approximately an average of 109.4° (H−C−O) and 124.4° (H−C═O).

The optimized parameters of the C_1 acyclic transition state (Figure 3b) are considered in contrast to the acyclic and cyclic minima. The C−H bond distance exhibits no significant changes among these three structures, while the O−H parameter decreases by a few hundreths of an angstrom in both the donor and acceptor compared to both minimum structures. The C═O bond distance decreased as compared to both minima but more significantly as compared to the C_{2h} dimer (0.13 Å, acceptor; 0.14 Å, donor) than the C_s structure (0.005 Å, acceptor; 0.003 Å, donor). In both moieties, the C−O bond distance was about 0.02 Å longer than that in the cyclic dimer, but in the donor of the C_1 transition state, it was only about 0.006 Å longer than its counterpart in the acyclic dimer, while there was no significant change observed in this parameter moiety A in the two acyclic structures. The H−C═O bond angles of the acceptor and donor increased by about 2.7° and 2.2°, respectively, over the cyclic minimum but only by 0.65° (acceptor) and 0.5° (donor) over the acyclic minimum. In the acceptor, the O−C═O bond angle was wider than that in the C_s dimer by about 1° and more narrow than that in the C_{2h} dimer by about 2.4°. In the donor, the changes in this parameter were much less pronounced [∼0° (C_s) and 1.5° (C_{2h})]. At our best level, the following were predicted: r(O···H) = 1.835 Å, θ(C═O···H) = 124.0°, θ(O···H−O) = 170.4°, and τ(O−C═O···H) = 101.6°.

B. Mechanisms of Dimerization. Relative energies of the six structures studied at the B3LYP, MP2, MP2-R12, and CCSD(T) levels of theory are reported in Table 2. All energies in both tables are listed relative to two monomers of formic acid.

It has been long-held that the dimerization of formic acid is a synchronous process of two trans isomers of FAM coming together to form c-FAD. However, as a result of recent experimental findings,[42] the dimerization of FAD might proceed through a stepwise process, from two trans monomers to the acyclic minimum, through an acyclic transition state to the cyclic minimum.

In this scenario, the dissociation energy of the dimer and the barrier to the double proton transfer were predicted as outlined above. The results obtained with DFT, MP2, MP2-R12, and CCSD(T) single-point energies are shown in Figures 4−7. With the use of DFT, D_e is 15.2 kcal/mol and $\Delta E^\dagger$ is 6.5 kcal/mol. At the [MP2/TZ2P(f,d)+diff] level of theory, D_e for this mechanism is found to be 16.2 kcal/mol and $\Delta E^\dagger$ is 6.8 kcal/mol, and with the use of MP2-R12, these values are 16.1 and 7.1 kcal/mol, respectively. From the CCSD(T)/aug′-cc-pVTZ single-point energies at the MP2/TZ2P+diff optimized structures, D_e is 17.2 kcal/mol and $\Delta E^\dagger$ is 8.4 kcal/mol, respectively. The counterpoise correction decreases the dissociation energy by 2.4−14.8 kcal/mol, which is in good agreement with the results obtained using the MP2-R12 method. While it is known that ab initio predictions of barrier heights are sensitive to basis set size and inclusion of correlation energy, it is found here that CCSD(T) predicts a barrier height of the double proton transfer in FAD that is about 1.5 kcal/mol greater than that found using the explicitly correlated MP2 method, but DFT is able to

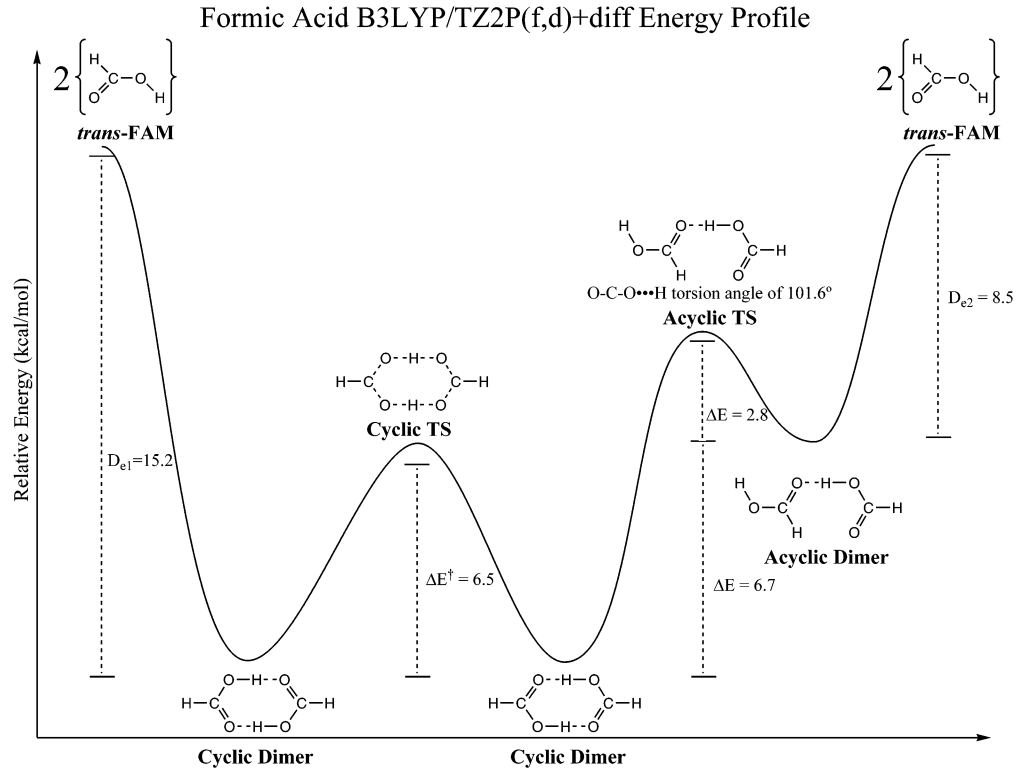

Figure 4. B3LYP energy profile for the formic acid dimer. Relative energies are in kcal/mol. D_{e1} is the dissociation energy of the cyclic dimer, and D_{e2} is the dissociation energy of the acyclic dimer. $\Delta E^{\dagger}$ is the barrier to double proton transfer in the cyclic dimer.

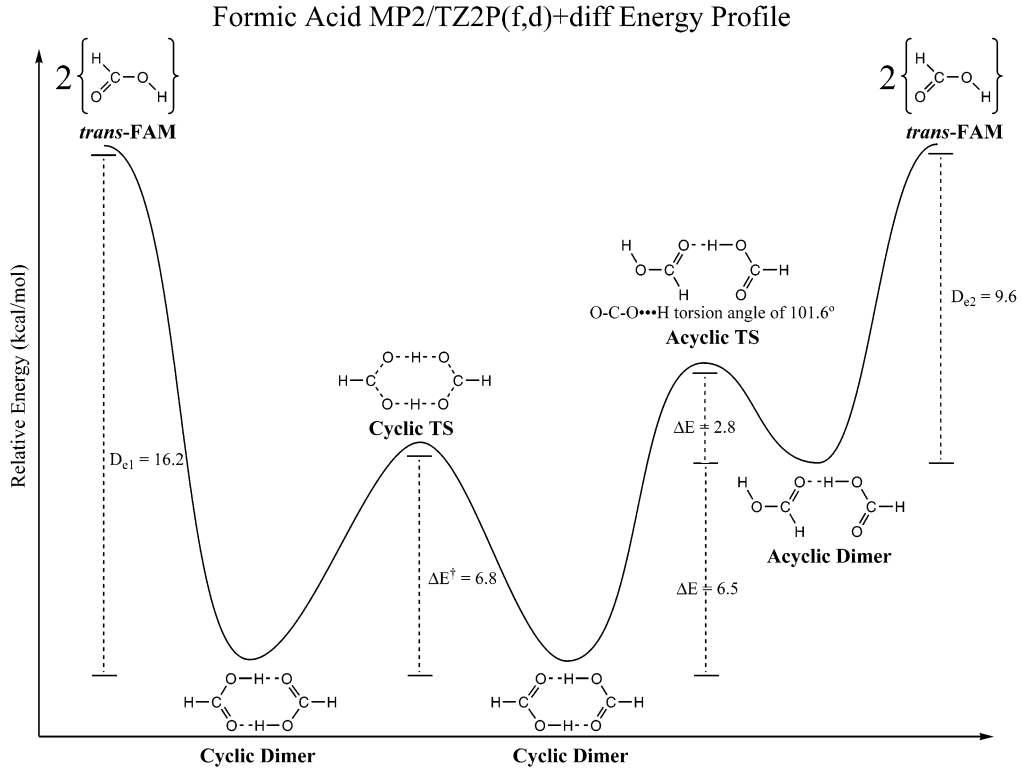

Figure 5. MP2 energy profile for the formic acid dimer. Relative energies are in kcal/mol. D_{e1} is the dissociation energy of the cyclic dimer, and D_{e2} is the dissociation energy of the acyclic dimer. $\Delta E^{\dagger}$ is the barrier to double proton transfer in the cyclic dimer.

produce a barrier height for this process that is within 0.5 kcal/mol of the result obtained via MP2-R12.

It should be noted here that proton tunneling in FAD is significant; Loerting and Liedl[72] reported that more than half of the hydrogenic motion in the double proton transfer of FAD occurs in the classically forbidden tunneling region, even at ambient temperatures. Interested readers are directed to ref 72.

The energy of stabilization from the acyclic to cyclic dimer, the barrier to this process, and the dissociation energy from the acyclic dimer (D_{e2}) to two monomers were calculated as previously described. DFT predicts these values as 6.7, 2.8, and

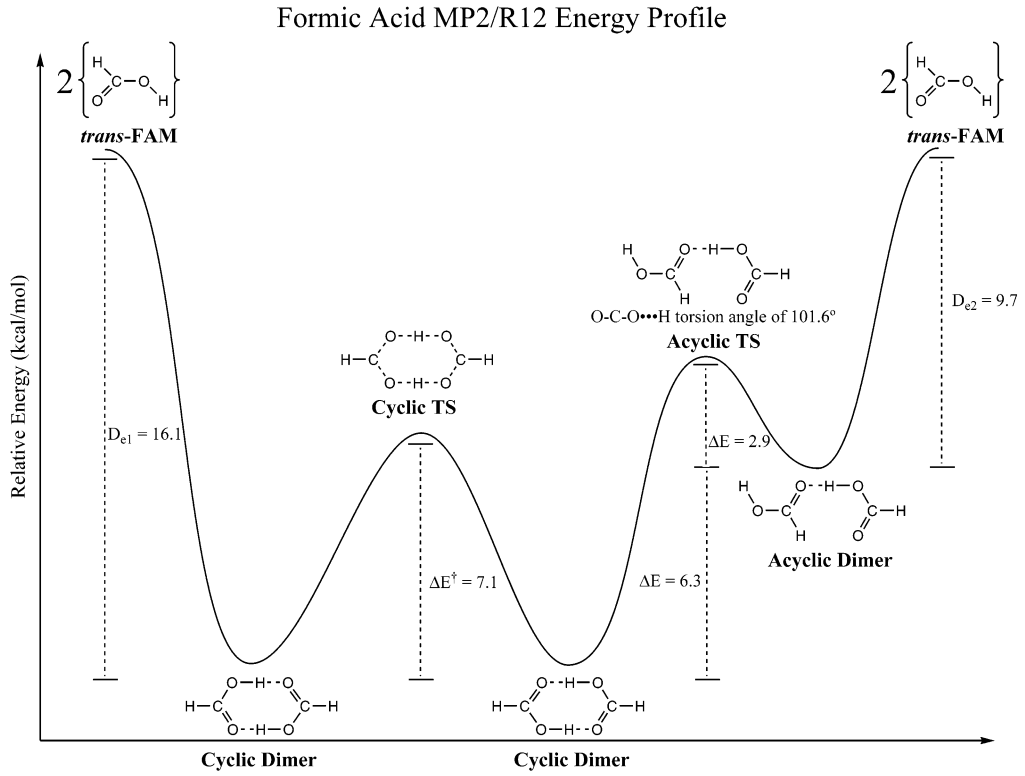

Figure 6. MP2-R12 energy profile for the formic acid dimer. Relative energies are in kcal/mol. D_{e1} is the dissociation energy of the cyclic dimer, and D_{e2} is the dissociation energy of the acyclic dimer. $\Delta E^{\dagger}$ is the barrier to double proton transfer in the cyclic dimer.

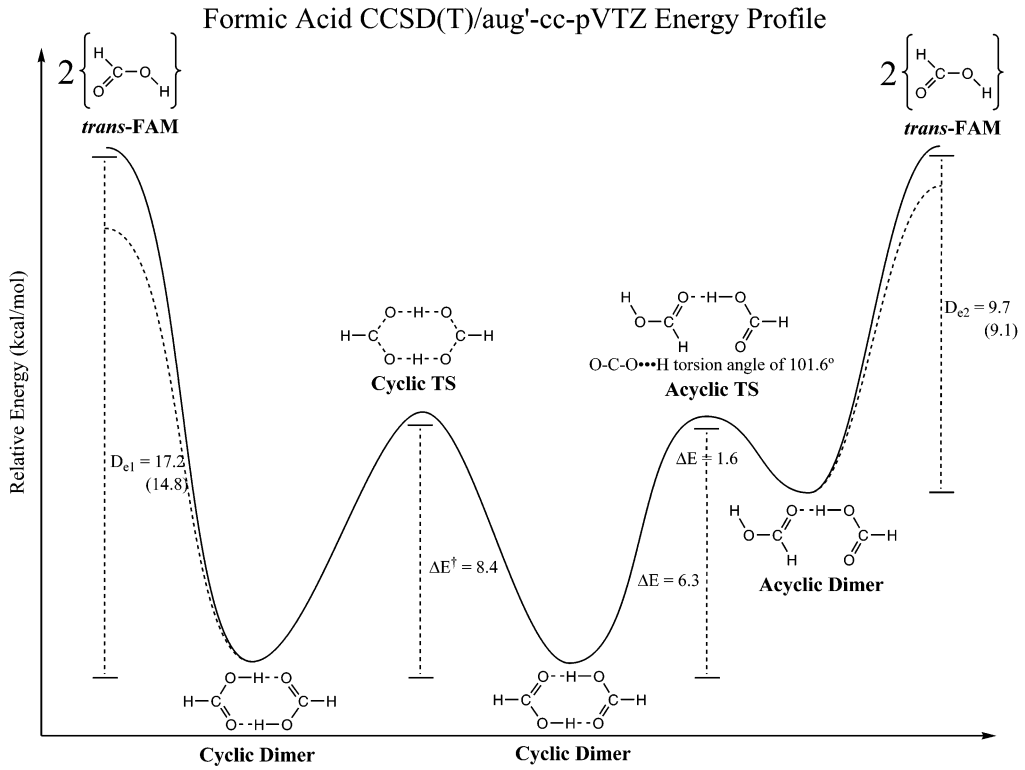

Figure 7. Energy profile of CCSD(T)/aug′-cc-pVTZ energy points at the MP2/TZ2P+diff optimized structures of the formic acid dimer. Relative energies are in kcal/mol. D_{e1} is the dissociation energy of the cyclic dimer, and D_{e2} is the dissociation energy of the acyclic dimer. $\Delta E^{\dagger}$ is the barrier to double proton transfer in the cyclic dimer. The counterpoise corrections are indicated by the dashed curves.

8.5 kcal/mol, respectively. At the MP2/TZ2P(f,d)+diff level of theory, the energy of stabilization is predicted to be 6.5 kcal/mol. ΔE is predicted as 2.8 kcal/mol, and D_{e2} is 9.6 kcal/mol. At the MP2-R12 level of theory, these values are 6.3, 2.9, and 9.7 kcal/mol, respectively. The CCSD(T) method yielded D_{e2} = 9.7 kcal/mol, and with the counterpoise correction, this value is decreased to 9.1 kcal/mol. The barrier to rotation at this level of theory is 1.6 kcal/mol, which is about half what is predicted by our best MP2 level of theory (2.9 kcal/mol at MP2-R12/K2). At the CCSD(T)/aug′-cc-pVTZ level, the cyclic dimer is 6.3 kcal/mol more stable than the acyclic minimum. While this energy difference is in excellent agreement with the value found

using MP2-R12, DFT matches the MP2-R12 values for the barrier to rotation better than CCSD(T).

A two-center collision is necessary for the formation of a single hydrogen bond followed by a rotation about the C═O bond and a second two-center approach to form the second hydrogen bond. The concerted double-hydrogen bond formation, however, requires a four-center encounter. Given that a two-center collision is statistically more probable than a four-center collision, and that the barrier to rotation is a mere 1.6 kcal/mol, it is suggested here that the dimerization of c-FAD proceeds through the stepwise mechanism.

Conclusions

At the MP2-R12/K2 level of theory, the direct dissociation energy of FAD is predicted to be 16.1 kcal/mol, and the barrier to the double proton transfer is predicted to be 7.1 kcal/mol. The cyclic minimum is 6.3 kcal/mol more stable than the acyclic minimum, and barrier to rotation about the C═O bond is 2.9 kcal/mol. The dissociation energy from the acyclic dimer is 9.7 kcal/mol. DFT reproduces these values reasonably well while CCSD(T) predicts a higher barrier to double proton transfer by about 1 kcal/mol and a lower barrier to rotation by a factor of 2. The counterpoise correction makes a significant difference of 2.4 kcal/mol for direct dissociation and about 0.6 kcal/mol for dissociation from the acyclic dimer.

Acknowledgment. Appreciation is expressed to Professor Wolfram Sander (Ruhr-Universitaet Bochum, Bochum, Germany) for communication about the acyclic transition state structure. Professors David L. Powell and Donald T. Jacobs (The College of Wooster, Wooster, Ohio) are also recognized for their insights and helpful discussions. N.R.B. also thanks Jason Gonzales and Damian Moran for their technical assistance and Wesley Allen for helpful scientific discussions. Edward Valeev and Joseph Kenny carried out the MP2-R12 computations. The research at the University of Georgia was supported through the SciDAC and Combustion programs of the U.S. Department of Energy. We gratefully acknowledge computational support from the DOE Pacific Northwest National Laboratory.

Supporting Information Available: Table of experimental and calculated vibrational frequencies from trans-FAM, c-FAD, a-FAD, and the cyclic and acyclic transition states. This material is available free of charge via the Internet at http://pubs.acs.org.

References and Notes

(1) Bender, M. L. *Mechanisms of Homogeneous Catalysis from Protons to Proteins*; John Wiley and Sons: New York, 1971.
(2) Melander, L.; Saunders, W. H. J. *Reaction Rates of Isotopic Molecules*; John Wiley and Sons: New York, 1980.
(3) Spinner, E. J. *Croat. Chim. Acta* **1982**, *55*, 249.
(4) Spinner, E. J. *J. Am. Chem. Soc.* **1983**, *105*, 756.
(5) Perrin, C. L.; Thoburn, J. D. *J. Am. Chem. Soc.* **1989**, *111*, 8010.
(6) Speakman, J. C. *Struct. Bonding* **1972**, *12*, 141.
(7) Emsley, J. *J. Chem. Soc. Rev.* **1980**, *9*, 91.
(8) Emsley, J.; Hoyte, O. P. A.; Overill, R. E. *J. Am. Chem. Soc.* **1978**, *100*, 3303.
(9) Scherer, G.; Limbach, H.-H. *J. Am. Chem. Soc.* **1989**, *111*, 5946.
(10) Scherer, G.; Limbach, H.-H. *J. Am. Chem. Soc.* **1994**, *116*, 1230.
(11) Meschede, L.; Limbach, H.-H. *J. Phys. Chem.* **1991**, *95*, 10267.
(12) Schlabach, M.; Limbach, H.-H.; Bunnenberg, E.; Shu, A. Y. L.; Tolf, B.-R.; Djerassi, C. *J. Am. Chem. Soc.* **1993**, *115*, 4554.
(13) Kohanoff, J.; Koval, S.; Estrin, D. A.; Laria, D.; Abashkin, Y. *J. Chem. Phys.* **2000**, *112*, 9498.
(14) Hrouda, V.; Florian, J.; Polasek, M.; Hobza, P. *J. Phys. Chem.* **1994**, *98*, 4742.
(15) Császár, A. G. *J. Am. Chem. Soc.* **1992**, *114*, 9569.
(16) Hu, C.-H.; Shen, M.; Schaefer, H. F. *J. Am. Chem. Soc.* **1993**, *115*, 2923.
(17) Császár, A. G. *J. Phys. Chem.* **1996**, *100*, 3541.
(18) Nahringbauer, I. *Acta Crystallogr. B* **1978**, *34*, 315.
(19) Albinati, A.; Rouse, K. D.; Thomas, M. W. *Acta Crystallogr. B* **1978**, *34*, 2188.
(20) Kwei, G.; Curl, R. *J. Chem. Phys.* **1960**, *32*, 1592.
(21) Almenningen, A.; Bastiansen, O.; Motzfeld, T. *Acta Chem. Scand.* **1969**, *23*, 2848.
(22) Almenningen, A.; Bastiansen, O.; Motzfeld, T. *Acta Chem. Scand.* **1970**, *24*, 747.
(23) Hocking, W. H. *Z. Naturforsch.* **1976**, *31a*, 1113.
(24) Hocking, W. H.; Winnewisser, G. *Z. Naturforsch.* **1976**, *31a*, 995.
(25) Winnewisser, B. P.; Hocking, W. H. *J. Phys. Chem.* **1980**, *84*, 1771.
(26) Miyazawa, T.; Pitzer, K. S. *J. Chem. Phys.* **1959**, *30*, 1076.
(27) Jakobsen, R. J.; Mikawa, Y.; Brasch, J. W. *Spectrochim. Acta* **1967**, *23A*, 2199.
(28) Makamoto, K.; Kishida, S. *J. Chem. Phys.* **1964**, *30*, 1076.
(29) Császár, A. G.; Allen, W. D.; Schaefer, H. F. *J. Chem. Phys.* **1998**, *108*, 9751.
(30) Costain, C. C.; Srivastava, G. P. *J. Chem. Phys.* **1964**, *41*, 1620.
(31) Bertie, J. E.; Michaelian, K. H.; Eysel, H. H. *J. Chem. Phys.* **1986**, *85*, 4779.
(32) Bertie, J. E.; Michaelian, K. H. *J. Chem. Phys.* **1982**, *76*, 886.
(33) Millikan, R. C.; Pitzer, K. S. *J. Am. Chem. Soc.* **1958**, *80*, 3515.
(34) Lazaar, K. I.; Bauer, S. H. *J. Am. Chem. Soc.* **1985**, *107*, 3769.
(35) Karpfen, A. *J. Chem. Phys.* **1984**, *88*, 415.
(36) Agranat, I.; Riggs, N. V.; Radom, L. *J. Chem. Soc., Chem. Commun.* **1970**, *2*, 80.
(37) Svensson, P.; Bergman, N.-A.; Ahlberg, P. *J. Chem. Soc., Chem. Commun.* **1990**, *12*, 862.
(38) Tsuzuki, S.; Uchimaru, T.; Matsumura, K.; Mikami, M.; Tanabe, K. *J. Chem. Phys.* **1999**, *110*, 11906.
(39) Graf, F.; Meyer, R.; Ha, T.-K.; Ernst, R. R. *J. Chem. Phys.* **1981**, *75*, 2914.
(40) Hayashi, S.; Umemura, J.; Kato, S.; Morokuma, K. *J. Phys. Chem.* **1984**, *88*, 1330.
(41) Kim, Y. *J. Am. Chem. Soc.* **1996**, *118*, 1522.
(42) Gantenberg, M.; Halupka, M.; Sander, W. *Chem.—Eur. J.* **2000**, *6*, 1865.
(43) Turi, L. *J. Phys. Chem.* **1996**, *100*, 11285.
(44) Frisch, M. J.; Trucks, G. W.; Schlegel, H. B.; Gill, P. M. W.; Johnson, B. G.; Robb, M. A.; Cheeseman, J. R.; Keith, T.; Petersson, G. A.; Montgomery, J. A.; Raghavachari, K.; Al-Laham, M. A.; Zakrzewski, V. G.; Ortiz, J. V.; Foresman, J. B.; Cioslowski, J.; Stefanov, B. B.; Nanayakkara, A.; Challacombe, M.; Peng, C. Y.; Ayala, P. Y.; Chen, W.; Wong, M. W.; Andres, J. L.; Replogle, E. S.; Gomperts, R.; Martin, R. L.; Fox, D. J.; Binkley, J. S.; Defrees, D. J.; Baker, J.; Stewart, J. P.; Head-Gordon, M.; Gonzalez, C.; Pople, J. A. *Gaussian 94*, revision C.3; Gaussian, Inc.: Pittsburgh, PA, 1995.
(45) Stanton, J. F.; Gauss, J.; Watts, J. D.; Nooijen, M.; Oliphant, N.; Perera, S. A.; Szalay, P. G.; Lauderdale, W. J.; Gwaltney, S. R.; Beck, S.; Balkova, A.; Bernholdt, D. E.; Baeck, K. K.; Rozyczko, P.; Sekino, H.; Hober, C.; Bartlett, R. J. *ACES II, a program product of the Quantum Theory Project*; University of Florida. Integral packages included are *VMOL* (Almlöf, J. and Taylor, P. R.); *VPROPS* (P. R. Taylor); *ABACUS* (Helgaker, T., Jensen, H. J. A., Jörgensen, P., Olsen, J., and Taylor, P. R.).
(46) Harrison, R. J.; Nichols, J. A.; Straatsma, T. P.; Dupuis, M.; Bylaska, E. J.; Fann, G. I.; Windus, T. L.; Apra, E.; de Jong, W.; Hirata, S.; Hackler, M. T.; Anchell, J.; Bernholdt, D.; Borowski, P.; Clark, T.; Clerc, D.; Dachsel, H.; Deegan, M.; Dyall, K.; Elwood, D.; Fruchtl, H.; Glendening, E.; Gutowski, M.; Hirao, K.; Hess, A.; Jaffe, J.; Johnson, B.; Ju, J.; Kendall, R.; Kobayashi, R.; Kutteh, R.; Lin, Z.; Littlefield, R.; Long, X.; Meng, B.; Nakajima, T.; Nieplocha, J.; Niu, S.; Rosing, M.; Sandrone, G.; Stave, M.; Taylor, H.; Thomas, G.; van Lenthe, J.; Wolinski, K.; Wong, A.; Zhang, Z. *NWChem, A Computational Chemistry Package for Parallel Computers*, version 4.1; Pacific Northwest National Laboratory: Richland, WA, 2002.
(47) Huzinaga, S. *J. Chem. Phys.* **1965**, *42*, 1293.
(48) Dunning, T. H. *J. Chem. Phys.* **1970**, *53*, 2823.
(49) Lee, T. J.; Schaefer, H. F. *J. Chem. Phys.* **1985**, *83*, 1784.
(50) Tschumper, G. S.; Schaefer, H. F. *J. Chem. Phys.* **1997**, *107*, 2529.
(51) Dunning, T. H. *J. Chem. Phys.* **1971**, *55*, 716.
(52) Møller, C.; Plesset, M. S. *Phys. Rev.* **1934**, *46*, 618.
(53) Pople, J. A.; Binkley, J. S.; Seeger, R. *Int. J. Quantum Chem. Symp.* **1976**, *10*, 1.
(54) Becke, A. D. *J. Chem. Phys.* **1993**, *98*, 5648.
(55) Lee, C.; Yang, W.; Parr, R. G. *Phys. Rev. B* **1988**, *37*, 785.
(56) Raghavachari, K.; Trucks, G. W.; Pople, J. A.; Head-Gordon, M. *Chem. Phys. Lett.* **1989**, *157*, 479.
(57) Bartlett, R. J.; Watts, J. D.; Kucharski, S. A.; Noga, J. *Chem. Phys. Lett.* **1990**, *165*, 513.
(58) Bartlett, R. J.; Watts, J. D.; Kucharski, S. A.; Noga, J. *Chem. Phys. Lett.* **1990**, *167*, 609.

(59) Gauss, J.; Lauderdale, W. J.; Stanton, J. F.; Watts, J. D.; Bartlett, R. J. *Chem. Phys. Lett.* **1991**, *182*, 207.
(60) Dunning, T. H. *J. Chem. Phys.* **1989**, *90*, 1007.
(61) Kendall, R. A.; Dunning, T. H.; Harrison, R. J. *J. Chem. Phys.* **1992**, *96*, 7696.
(62) Boys, S. F.; Bernardi, F. *Mol. Phys.* **1970**, *19*, 553.
(63) Kutzelnigg, W.; Klopper, W. *J. Chem. Phys.* **1991**, *94*, 1985.
(64) Klopper, W. *Chem. Phys. Lett.* **1991**, *186*, 583.
(65) Valeev, E. F.; Schaefer, H. F. *J. Chem. Phys.* **2000**, *113*, 3990.
(66) Crawford, T. D.; Sherrill, C. D.; Valeev, E. F.; Fermann, J. T.; Leininger, M. L.; King, R. A.; Brown, S. T.; Janssen, C. L.; Seidl, E. T.; Yamaguchi, Y.; Allen, W. D.; Xie, Y.; Vacek, G.; Hamilton, T. P.; Kellogg, C. B.; Remington, R. B.; Schaefer, H. F. *PSI 3.0*; PSITECH, Inc.: Watkinsville, GA, 2000.
(67) Klopper, W.; Noga, J. *J. Chem. Phys.* **1995**, *103*, 6127.
(68) Richardson, N. A.; Rienstra-Kiracofe, J. C.; Schaefer, H. F. *J. Am. Chem. Soc.* **1999**, *121*, 10813.
(69) Richardson, N. A.; Rienstra-Kiracofe, J. C.; Schaefer, H. F. *Inorg. Chem.* **1999**, *38*, 6271.
(70) Goddard, J. D.; Yamaguchi, Y.; Schaefer, H. F. *J. Chem. Phys.* **1992**, *96*, 1158.
(71) Chang, Y.-T.; Yamaguchi, Y.; Miller, W. H.; Schaefer, H. F. *J. Am. Chem. Soc.* **1987**, *109*, 7245.
(72) Loerting, T.; Liedl, K. R. *J. Am. Chem. Soc.* **1998**, *120*, 12595.
(73) Harmony, M. D.; Laurie, V. W.; Kuczkowski, R. L.; Schwendeman, R. H.; Ramsay, D. A.; Lovas, F. J.; Lafferty, W. J.; Maki, A. G. *J. Phys. Chem. Ref. Data* **1979**, *8*, 619.